Osmium Tetrafluoride Dioxide, *cis*-OsO_2F_4

Karl O. Christe,*,† David A. Dixon,‡ Hans Georg Mack,§ Heinz Oberhammer,§ Alain Pagelot,∥ Jeremy C. P. Sanders,⊥ and Gary J. Schrobilgen⊥

Contribution from Rocketdyne, A Division of Rockwell International Corporation, Canoga Park, California 91309, Central Research and Development Department, E.I. du Pont de Nemours and Company, Inc., Experimental Station, Wilmington, Delaware 19880, Institut für Physikalische und Theoretische Chemie, Universität Tübingen, 7400 Tübingen, Germany, Department of Chemistry, McMaster University, Hamilton, Ontario L8S 4MI, Canada, and Bruker Spectrospin, G7160 Wissembourg, France

Received June 24, 1993®

Abstract: The new osmium(VIII) oxo fluoride obtained from the reaction of KrF_2 and OsO_4 in anhydrous HF solution and originally identifed as $OsOF_6$ is shown by quantitative material balance, electron diffraction, NMR and vibrational spectroscopy, and density functional theory calculations to be *cis*-OsO_2F_4. The combined electron diffraction study and DFT calculations result in the following geometry: $r_{Os=O}$ = 1.674(4) Å, r_{Os-F_e} = 1.883(3) Å, r_{Os-F_a} = 1.843(3) Å, ∠O=Os=O = 103.5(25)°, $\angle F_e$–Os–F_e = 77.3(26)°, $\angle F_a$–Os–F_a = 172.0(3)°, ∠O=Os–F_a = 92.4(17)°. In addition to the ^{19}F NMR spectrum, the ^{187}Os chemical shift was measured for *cis*-OsO_2F_4 from its $^{19}F\{^{187}Os\}$ inverse correlation spectrum. The results from the density functional theoretical calculations show that for OsO_2F_4 the *cis*-structure of C_{2v} symmetry is a true minimum and that, in accord with expectations for a d^0 transition metal complex, the *trans*-D_{4h} structure is not a minimum energy structure and distorts to a C_{2v} structure.

Introduction

The synthesis of novel fluorides at the limits of oxidation and coordination is a great challenge. Of particular interest in this respect is osmium because from its oxide chemistry this element is known to possess a rare maximum oxidation state of +VIII. Although the replacement of one doubly bonded oxygen ligand by two singly bonded fluorine ligands does not alter the formal oxidation state of the central atom, such a replacement becomes increasingly more difficult with an increasing number of fluorine ligands. Thus, the effective electron-withdrawing power of two singly bonded fluorine ligands is considerably greater than that of one doubly bonded oxygen ligand,[1] and steric crowding of ligands becomes a problem for coordination numbers in excess of 6.[2] Therefore, it is not surprising that, in the Os(VIII) series, OsF_8, $OsOF_6$, OsO_2F_4, OsO_3F_2, and OsO_4, until recently only OsO_4 and OsO_3F_2 had been known and well characterized.[3-5] Two years ago, Bougon reported[6] the synthesis of a new Os(VIII) oxo fluoride for which he proposed the composition $OsOF_6$. In a subsequent brief note[7] by Christe and Bougon, however, it was shown that this compound is *cis*-OsO_2F_4 and not $OsOF_6$. In this paper we present the experimental evidence for this new Os(VIII) oxo fluoride being indeed OsO_2F_4 and having a *cis*-structure.

Experimental Section

Materials and Apparatus. OsO_4 (Aldrich, 99.8%) was sublimed prior to use. KrF_2 was prepared by UV-photolysis of Kr in liquid F_2 at −196 °C using a stainless-steel reactor equipped with a sapphire window.[8] HF (Matheson) was dried by storage over BiF_5.[9]

Volatile materials were handled in a stainless-steel vacuum line equipped with Teflon-FEP U-traps, stainless-steel bellows-seal valves, and a Heise Bourdon tube-type pressure gauge.[10] The line and other hardware employed were passivated with ClF_3, BrF_5, and HF. Nonvolatile materials were handled in the dry nitrogen atmosphere of a glovebox.

Vibrational Spectra. Infrared spectra were recorded in the range 4000–200 cm^{-1} on a Perkin-Elmer Model 283 spectrophotometer. Spectra of solids were obtained by using dry powders pressed between AgCl windows in an Econo press (Barnes Engineering Co.). Spectra of gases were obtained by using a Teflon cell of 5-cm path length equipped with AgCl windows. Raman spectra were recorded on a Spex Model 1403 spectrophotometer using using the 647.1-nm exciting line of a Kr ion laser. Sealed quartz tubes were used as sample containers in the transverse-viewing–transverse-excitation mode. A previously described[11] device was used for recording the low-temperature spectra. For the HF solutions, thin-walled Kel-F tubes were used as sample tubes.

Nuclear Magnetic Resonance Spectroscopy. The ^{19}F NMR spectra were recorded unlocked (field drift <0.1 Hz h^{-1}) on a Bruker AM-500 spectrometer as previously described.[12] No line-broadening parameters were used in the exponential multiplication of the free induction decays prior to Fourier transformation.

The two-dimensional (^{19}F, ^{187}Os) inverse NMR spectra were run on a Bruker AMX-300 spectrometer equipped with a 7.0463-T cryomagnet. The spectra were obtained with a 5-mm triple resonance $^1H/^{31}P/X$ probe with the outer X coil tunable over a broad-band frequency range and the ^1H channel retuned to ^{19}F. The experiments were carried out using the phase-sensitive (TPPI) HMQC pulse sequence.[13,14] The ^{19}F dimension was generated with 8 K data points and a spectral width of 20 000 Hz, while the ^{187}Os dimension was generated with 115 data points and a

† Rocketdyne.
‡ E.I. du pont.
§ Universität Tübingen.
∥ Bruker Spectrospin.
⊥ McMaster University.
® Abstract published in *Advance ACS Abstracts*, October 15, 1993.

(1) Christe, K. O.; Dixon, D. A. *J. Am. Chem. Soc.* **1992**, *114*, 2978.
(2) Christe, K. O.; Curtis, E. C.; Dixon, D. A.; Mercier, H. P. A.; Sanders, J. C. P.; Schrobilgen, G. J.; Wilson, W. W. In *Fluorine and Fluorine-Containing Substituent Groups in Inorganic Chemistry*; Thrasher, J., Strauss, S., Eds.; ACS Symposium Series; American Chemical Society: in press.
(3) Hepworth, M. A.; Robinson, P. L. *J. Inorg. Nucl. Chem.* **1957**, *4*, 24.
(4) Nguyen-Nghi; Bartlett, N. *C. R. Acad. Sci. Paris Sect. C* **1969**, *269*, 756.
(5) Hope, E. G.; Levason, W.; Ogden, J. S. *J. Chem. Soc., Dalton Trans.* **1988**, 61 and 997.
(6) Bougon, R. *J. Fluorine Chem.* **1991**, *53*, 419.
(7) Christe, K. O.; Bougon, R. J. *Chem. Soc., Chem. Commun.* **1992**, 1056.
(8) Christe, K. O.; Wilson, W. W.; Bougon, R. A. *Inorg. Chem.* **1986**, *25*, 2163.
(9) Christe, K. O.; Wilson, W. W.; Schack, C. J. *J. Fluorine Chem.* **1978**, *11*, 71.
(10) Christe, K. O.; Wilson, R. D.; Schack, C. J. *Inorg. Synth.* **1986**, *24*, 3.
(11) Miller, F. A.; Harney, B. M. *Appl. Spectrosc.* **1969**, *23*, 8.
(12) Christe, K. O.; Dixon, D. A.; Mahjoub, A. R.; Mercier, H. P. A., Sanders, J. C. P.; Seppelt, K.; Schrobilgen, G. J.; Wilson, W. W. *J. Am. Chem. Soc.* **1993**, *115*, 2696.

0002-7863/93/1515-11279$04.00/0

spectral width of 27 777 Hz. The number of transients collected for each t_1 increment was 256. A recycling time of 2.2 s was used. The $1/2J$ delay was 8 ms. In the ^{187}Os dimension, the free induction decays were zero-filled to 2 K data points prior to Fourier transformation; no zero-filling was applied to free induction decays in the ^{19}F dimension. This gave data point resolutions of 27 Hz/point (^{187}Os) and 4.88 Hz/point (^{19}F). The data were processed using a 90° shifted sine bell in the ^{19}F dimension and a 60° sine bell in the ^{187}Os dimension.

The ^{19}F spectra were referenced to a neat external sample of $CFCl_3$ at ambient temperature. The ^{187}Os chemical shift was calculated from its absolute frequency using the conversion factor 6.850 099 8 MHz for $\delta(OsO_4) = 0.0$ ppm ($\Xi = 2.282\,343$ MHz). The chemical shift convention used is that a positive sign signifies a chemical shift to high frequency of the reference compound.

Samples were prepared in prepassivated 25-cm lengths of 4-mm o.d. FEP tubing, heat-sealed at one end and joined to a Kel-F valve. The *cis*-OsO_2F_4 (0.015 15 g, 0.050 81 mmol) was loaded into the tube in the drybox. The tube was transferred to a Teflon FEP metal vacuum line and anhydrous HF was distilled *in vacuo* into the tube at −78 °C to a depth of 3 cm. The tube was heat-sealed *in vacuo* while the contents were kept frozen at −196 °C. On warming of the sample to room temperature, a pale red saturated solution resulted which contained some solid *cis*-OsO_2F_4; this solution was decanted into the other end of the tube before the NMR spectrum was run.

Electron Diffraction. The electron diffraction intensities were recorded with a Gasdiffracktograph KD-G2[15] at two camera distances (25 and 50 cm) and with an accelerating voltage of about 60 kV. The electron wavelength was calibrated with ZnO diffraction patterns. The sample was sublimed at a reservoir temperature of 40 °C and the stainless-steel inlet system and nozzle with 0.5-mm diameter were heated to 50 °C. The photographic plates were analyzed by the usual methods.[16]

Synthesis of *cis*-OsO_2F_4. A $^3/_4$-in. o.d. Teflon-FEP U-trap that was closed by two stainless-steel valves was passivated, and OsO_4 (888.7 mg, 3.496 mmol) and dry HF (5.1027 g) were condensed in at −196 °C in a dynamic vacuum. In the same manner, KrF_2 (969.1 mg, 7.956 mmol) was added, and the resulting mixture was allowed to warm slowly toward room temperature. On warm up, gas evolution set in and the originally clear, colorless solution and solid OsO_4 phase turned orange-brown. To slow down the reaction, the reactor was intermittently cooled with a −78 °C bath when the gas evolution became too rapid. After completion of gas evolution, the solid product in the bottom of the reactor had turned purple. The gas evolution was measured by cooling the reactor first to −196 °C and then to −95 °C and measuring the amounts of noncondensible gas at each temperature by both *P*, *V*, *T* methods and by weight. The gas, noncondensible at −196 °C, was identified as oxygen (3.50 mmol), and that −95 °C as Kr (6.99 mmol). The combined weight loss was 696 mg (weight calculated for 3.496 mmol of O_2 and 6.992 mmol of Kr = 697.8 mg). The HF solvent and excess of KrF_2 were removed by pumping at −22 °C for 2 h leaving behind 1.047 g of a purple solid (weight calculated for 3.496 mmol of OsO_2F_4 = 1.043 g).

Computational Methods. The density functional theory (DFT)[17] calculations were done with the program DGauss,[18] which employs Gaussian orbitals on a Cray YMP computer. The initial basis set[19] for O and F is a polarized valence double-ζ set with the form (621/41/1) and a [7/3/3] fitting basis set. Norm-conserving pseudopotentials[20] were generated for Os following the work of Troullier and Martins.[21] The valence basis set for Os is (4,2/4/3,1) with a fitting basis set of [7/4/5]. The calculations were initially done at the local density functional (LDFT) level with the local potential of Vosko, Wilk, and Nusair.[22] Subsequently, the calculations were also done at the nonlocal level with the exchange potential of Becke[23] together with the nonlocal correlation functional of Perdew[24] (NLDFT/BP). For this case, a somewhat improved valence basis set of the form (721/51/1) was used for O and F. Geometries were optimized by using analytical gradients.[18] Second derivatives were calculated by numerical differentiation of the analytic first derivatives. A 2 point method with a finite difference of 0.01 au was used.

Results and Discussion

Synthesis and Properties of OsO_2F_4. The reaction of OsO_4 with KrF_2 in anhydrous HF solution proceeds quantitatively according to (1), as shown by an excellent material balance. Even

$$OsO_4 + 2KrF_2 \xrightarrow{HF} OsO_2F_4 + 2Kr + O_2 \qquad (1)$$

in the presence of a 2-fold excess of KrF_2 no further oxygen–fluorine exchange was observed, and the excess of KrF_2 was recovered unreacted. These results establish that the product from the OsO_4 + KrF_2 reaction is OsO_2F_4 and not $OsOF_6$ as previously reported.[6] The physical and spectroscopic properties of OsO_2F_4 (see below) are identical to those previously ascribed[6] to $OsOF_6$ and leave no doubt that the two products are identical. The facts that the reaction between KrF_2 and OsO_4 sets in at temperatures well below the incipient decomposition of KrF_2, that the yield of OsO_2F_4 based on KrF_2 is quantitative, and that under these conditions F_2 was shown to be unreactive with HF solutions of OsO_4 establish that reaction (1) involves a direct attack of KrF_2 on OsO_4 and does not proceed through an initial KrF_2 decomposition to F atoms which then react with OsO_4.

The OsO_2F_4 is a purple solid with a melting point of 90 °C and a vapor pressure of 1 Torr at room temperature. It can be stored at room temperature for extended time periods without significant decomposition. It dissolves in anhydrous HF to give purplish-red solutions. It hydrolyzes rapidly with formation of HF and a black precipitate. The X-ray powder pattern of OsO_2F_4 was identical to that previously ascribed[6] to $OsOF_6$.

Nuclear Magnetic Resonance Spectra. The ^{19}F NMR spectrum of a saturated solution of OsO_2F_4 in anhydrous HF shows two triplets of equal intensity characteristic of an A_2X_2 spin system (Figure 1). This provides definitive proof of the *cis* geometry adopted by OsO_2F_4, since the *trans*-isomer would have all four fluorine ligands equivalent and the ^{19}F NMR spectrum would only display a singlet arising from the A_4 spin system. The triplet multiplicities arise from the two-bond F_a–F_e coupling which has a value of 138.3 Hz. At present, it is difficult to make a definitive assignment as to which triplet arises from which fluorine ligand environment, i.e., F-*trans*-to-F (F_a) or F-*trans*-to-O (F_e). Comparison of the ^{19}F chemical shifts with those in the related octahedral species WOF_5^- [25] and $ReOF_5$,[26] where unambiguous assignment of the two environments can be made from the multiplicities of the resonances, suggests that the low-frequency triplet (δ = 15.8 ppm) should be ascribed to the F-*trans*-to-O

(13) Marion, D.; Wuthrich, K. *Biochem. Biophys. Res. Commun.* **1983**, *113*, 967. Bodenhausen, G.; Kogler, H.; Ernst, R. R. *J. Magn. Reson.* **1984**, *58*, 370.
(14) Bax, A.; Subramanian, S. J. *Magn. Reson.* **1986**, *67*, 565.
(15) Oberhammer, H. *Molecular Structure by Diffraction* Methods; The Chemical Society: London, 1976; Vol. 4, p 24.
(16) Oberhammer, H.; Gombler, W.; Willner, H. *J. Mol. Struct.* **1981**, *70*, 273.
(17) (a) Parr, R. G.; Yang, W. *Density Functional Theory of Atoms and Molecules*; Oxford University Press: New York, 1989. (b) Salahub, D. R. In *Ab Initio Methods in Quantum Chemistry-II*; Lawley, K. P., Ed.; J. Wiley & Sons: New York, 1987; p 447. (c) Wimmer, E.; Freeman, A. J.; Fu, C.-L.; Cao, P.-L.; Chou, S.-H.; Delley, B. In *Supercomputer Research in Chemistry and Chemical Engineering*; Jensen, K. F., Truhlar, D. G., Eds.; ACS Symposium Series No. 353; American Chemical Society: Washington, DC, 1987; p 49. (d) Jones, R. O.; Gunnarsson, O. *Rev. Mod. Phys.* **1989**, *61*, 689. (e) Zeigler, T. *Chem. Rev.* **1991**, *91*, 651.
(18) (a) Andzelm, J.; Wimmer, E.; Salahub, D. R. In *The Challenge of d and f Electrons: Theory and Computation*; Salahub, D. R., Zerner, M. C., Eds.; ACS Symposium Series No. 394; American Chemical Society: Washington, DC, 1989; p 228. (b) Andzelm, J. In *Density Functional Methods in Chemistry*; Ed. Labanowski, J., Andzelm, J., Eds.; Springer-Verlag: New York, 1991; p 101. (c) Andzelm, J.; Wimmer, E. *J. Chem. Phys.* **1992**, *96*, 1280. DGauss is a local density functional program available via the Cray Research Unichem Project, Cray Research, Eagan, MN, 1993.
(19) Godbout, N.; Salahub, D. R.; Andzelm, J.; Wimmer, E. *Can. J. Chem.* **1992**, *70*, 560.
(20) Chen, H.; Kraskowski, M.; Fitzgerald, G. *J. Chem. Phys.*, in press.
(21) Troullier, N.; Martins, J. L. *Phys. Rev. B* **1991**, *43*, 1993.
(22) Vosko, S. J.; Wilk, L.; Nusair, M. *Can. J. Phys.* **1980**, *58*, 1200.
(23) (a) Becke, A. D. *Phys. Rev. A* **1988**, *38*, 2098. (b) Becke, A. D. In *The Challenge of d and f Electrons: Theory and Computation*; Salahub, D. R., Zerner, M. C., Eds.; ACS Symposium Series No. 394; American Chemical Society: Washington, DC, 1989; p 166. (c) Becke, A. D. *Int. J. Quantum Chem. Quantum Chem. Symp.* **1989**, *23*, 599.
(24) Perdew, J. P. *Phys. Rev. B* **1986**, *33*, 8822.
(25) McFarlane, W.; Noble, A. M.; Winfield, J. M. *J. Chem. Soc. A* **1971**, 948.
(26) Bartlett, N.; Beaton, S.; Reeves, L. W.; Wells, E. J. *Can. J. Chem.* **1964**, *42*, 2531.

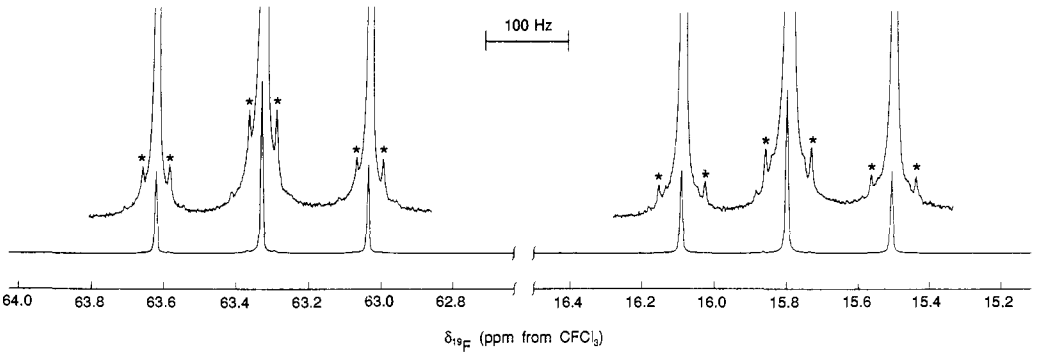

Figure 1. ^{19}F NMR spectrum (470.599 MHz) of a saturated solution of *cis*-OsO_2F_4 in anhydrous HF at 30 °C. The vertical expansion (×32) clearly reveals the satellites (denoted by asterisks) arising from spin coupling of the two ^{19}F ligand environments to natural-abundance (1.64%) ^{187}Os.

environment and the high-frequency triplet (δ = 63.3 ppm) to the F-*trans*-to-F environment. In addition, the ^{19}F chemical shifts of the *cis*-$WO_2F_4^{2-}$ anion have also previously been assigned with the F-*trans*-to-F environment to high frequency of the F-*trans*-to-O environment.[27] On the other hand, coupling constant considerations indicate that the assignments for *cis*-OsO_2F_4 should be the reverse of those given above. Since the F_e–Os bonds are, as a consequence of F_e being *trans* to the stronger π-donor oxygen ligand, longer and more polar than the F_a–Os bonds, the $^1J(^{19}F_e$–$^{187}Os)$ coupling would be expected to be smaller than $^1J(^{19}F_a$–$^{187}Os)$ coupling (*vide infra*). On this basis, the F_e environment would be assigned to the high-frequency triplet and the F_a environment to the low-frequency triplet. A similar ambiguity also exists for the assignment of the F_a and F_e environments in the *cis*-$ReO_2F_4^-$ [28] and *cis*-$TcO_2F_4^-$ [29] anions, and the problem is currently under further investigation.

At high gain, each component of the two triplets displays low-intensity satellites (Figure 1), which arise from ^{19}F coupling to the low-abundance (1.64%) spin-active isotope ^{187}Os (I = $^1/_2$). The satellites yield two couplings, viz., $^1J(^{19}F_{lf}$–$^{187}Os)$ = 35.1 Hz and $^1J(^{19}F_{hf}$–$^{187}Os)$ = 59.4 Hz, for the low-frequency and high-frequency resonances, respectively, which represent the first reported couplings between ^{187}Os and ^{19}F. As discussed above, the actual assignment as to which fluorine ligand environment gives rise to which coupling constant is not yet resolved.

Osmium-187 is the least sensitive nuclide (receptivity with respect to ^{13}C = 1.15 × 10^{-3}) in the Periodic Table, and its observation by conventional NMR techniques is very difficult.[30] Indeed until very recently, the only known ^{187}Os chemical shifts were of the standard, OsO_4,[31] and a few μ-hydrido dinuclear osmium clusters.[32] In 1990, Benn and co-workers[33] obtained ^{187}Os NMR parameters [viz., $\delta(^{187}Os)$, $T_1(^{187}Os)$, $^1J(^{187}Os$–$^{31}P)$, and $^1J(^{187}Os$–$^1H)$] from a range of organo–osmium compounds by use of indirect 2D NMR spectroscopy in which the sensitive ^1H or ^{31}P nuclides were used for observation.

In view of the success of these experiments, it seemed worthwhile to attempt the acquisition of the ^{187}Os NMR spectrum of *cis*-OsO_2F_4 by indirect methods with ^{19}F as the observation nuclide. Hitherto, ^{19}F had only been used in the inverse detection of ^{13}C and ^{183}W.[34] The standard $^{19}F\{^{187}Os\}$ inverse correlation spectrum obtained for a saturated solution of *cis*-OsO_2F_4 in anhydrous HF clearly reveals a correlation with the ^{187}Os dimension and gives the ^{187}Os chemical shift of *cis*-OsO_2F_4 as 1431 ± 10 ppm with respect to OsO_4. This experiment uses multiplet quantum transitions which result in the loss of the passive heteronuclear couplings in the ^{187}Os dimension.[35] So far, attempts to obtain a spectrum by means of a double INEPT inverse experiment,[36] which should have the ^{19}F multiplicity manifest in the ^{187}Os dimension, have been unsuccessful. The ^{187}Os chemical shift of *cis*-OsO_2F_4 is the first to be reported for an Os(VIII) oxo fluoride and is strongly deshielded with respect to OsO_4. The only other precedent for this situation is found in ^{99}Tc NMR spectroscopy, where the chemical shift of the *cis*-$TcO_2F_4^-$ anion is deshielded with respect to the corresponding tetraoxo-species TcO_4^-,[29] although chemical shifts of metal nuclei, such as ^{99}Tc, do not correlate well with the electronegativity of the substituents.[37]

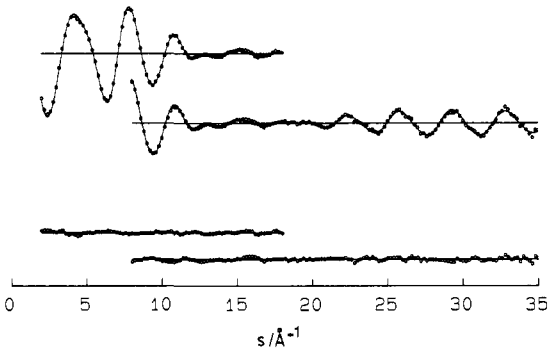

Figure 2. Experimental (dots) and calculated (solid line) molecular intensities and differences for *cis*-OsO_2F_4.

Electron Diffraction Analysis. The observed molecular intensities in the *s*-ranges 2–18 and 8–35 Å^{-1} at intervals of Δs = 0.2 Å^{-1} are shown in Figure 2. The radial distribution function of OsO_2F_4 (Figure 3) was calculated by Fourier transform of the molecular intensities by applying an artificial damping function $\exp(-\gamma s^2)$ with γ = 0.002 Å^2. In the least-squares refinements the molecular intensities were modified by a digonal weight matrix, and known scattering amplitudes and phases were used.[38] The electron diffraction analysis of OsO_2F_4 presents two major problems: (1) The equatorial and axial Os–F bond lengths are

(27) Buslaev, Yu. A.; Petrosynants, S. P. *J. Struct. Chem.* (*Engl. Transl.*) **1969**, *10*, 983.
(28) (a) Bol'shakov, A. M.; Glushkova, M. A.; Buslaev, Yu. A. *Dokl. Chem.* (*Engl. Transl.*) **1983**, *273*, 417. (b) Casteel, W. J., Jr.; LeBlond, N.; Mercier, H. P. A.; Schrobilgen, G. J. Unpublished results.
(29) (a) Mercier, H. P. A.; Schrobilgen, G. *J. Inorg. Chem.* **1993**, *32*, 145. (b) Casteel, W. J., Jr.; LeBlond, N.; Lock, P. E.; Schrobilgen, G. J. Unpublished results.
(30) Goodfellow, R. J. In *Multinuclear* NMR; Mason, J., Ed.; Plenum Press: New York, 1987; Chapter 20, pp 521–561.
(31) Schwenk, A. *Prog. NMR Spectrosc.* **1985**, *17*, 69. Schwenk, A. *Z. Phys.* **1968**, *213*, 482. Kaufmann, J.; Schwenk, A. *Phys. Lett.* **1967**, *24A*, 115.
(32) Cabeza, J. A.; Mann, B. E.; Maitlis, P. M.; Brevard, C. *J. Chem. Soc., Dalton Trans.* **1988**, 629. Cabeza, J. A.; Nutton, A.; Mann, B. E.; Brevard, C.; Maitlis, P. M. *Inorg. Chim. Acta* **1986**, *115*, 447. Cabeza, J. A.; Mann, B. E.; Brevard, C.; Maitlis, P. M. *J. Chem. Soc., Chem. Commun.* **1985**, 65.
(33) (a) Benn, R.; Brenneke, H.; Joussen, E.; Lehmkuhl, H.; Ortiz, F. L. *Organometallics* **1990**, *9*, 756. (b) Benn, R.; Joussen, E.; Lehmkuhl, H.; Ortiz, F. L.; Rufinska, A. *J. Am. Chem. Soc.* **1989**, *111*, 8754.
(34) Bourdonneau, M.; Brevard, C. *Inorg. Chem.* **1990**, *29*, 3270.
(35) Müller, L. *J. Am. Chem. Soc.* **1979**, *101*, 4481. Bax, A.; Griffey, R. H.; Hawkins, B. L. *J. Am. Chem. Soc.* **1983**, *105*, 7188. Bax, A.; Griffey, R. H.; Hawkins, B. L. *J. Magn. Reson.* **1983**, *55*, 301. Müller, L.; Schiksius, R. A.; Opella, S. J. *J. Magn. Reson.* **1986**, *66*, 379.
(36) Bodenhausen, G.; Ruben, D. J. *Chem. Phys. Lett.* **1980**, *69*, 185. Benn, R.; Brenneke, H.; Frings, A.; Lehmkuhl, H.; Mehler, G.; Rufinska, A.; Wildt, T. *J. Am. Chem. Soc.* **1988**, *110*, 5661.
(37) One of the reviewers has pointed out that the chemical shift of ^{99}Tc in TcO_3CH_3 is substantially downfield from that in TcO_3F.

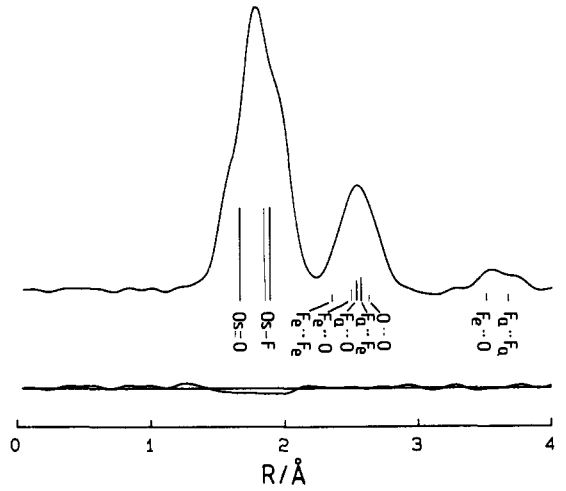

Figure 3. Experimental radial distribution function and difference curve. The positions of interactomic distances are indicated by vertical lines.

Table I. Results of Electron Diffraction Analyses and Theoretical Calculations

Geometric Parameters

	electron diffraction[a]		
	model I	model II	theoretical
Os=O	1.674(4)	1.674(4)	1.724
$(Os-F)_{mean}$	1.863(3)	1.863(3)	1.901
$(Os-F_e)-(Os-F_a)$	0.000[b]	0.040[b]	0.040
$Os-F_e$	1.863(3)[c]	1.883(3)	1.921
$Os-F_a$	1.863(3)[c]	1.843(3)	1.881
O=Os=O	97.4(56)	103.5(25)	102.6
F_e-Os-F_e	78.5(21)	77.3(26)	78.6
$F_e-Os=O$	92.1(39)[c]	89.6(16)[c]	89.4
F_e-Os-F_a	85.5(12)	87.0(15)	85.0
$O=O-F_a$	93.8(8)[c]	92.4(17)[c]	94.1
F_a-Os-F_a	168.6(30)[c]	172.0(35)[c]	169.0

Interatomic Distances and Vibrational Amplitudes for Model II

	r	l		r	l
Os=O	1.674(4)	0.046(4)	$F_e..F_e$	2.35(7)	
Os-F	1.863(3)	0.054(3)	$O..F_e$	2.51(4)	
$F_e..O$	3.53(1)	0.080(27)	$O..F_a$	2.54(4)	0.110[b]
$F_a..F_a$	3.68(1)		$F_a..F_e$	2.57(4)	
			O..O	2.63(5)	

[a] r_a distances in Å and angles in deg. Error limits are 3σ values. [b] Not refined. [c] Dependent geometric parameter.

very similar and cannot be determined separately. A mean value $(Os-F)_{mean} = {}^1/_2[(Os-F_e) + (Os-F_a)]$ was refined, and the bond length difference $(Os-F_e)-(Os-F_a)$ was set either to zero (model I) or to the theoretically calculated value of 0.040 Å (model II). (2) In near-octahedral structures all short nonbonded distances, which form the peak near 2.56 Å in our radial distribution function, are closely spaced and their assignment is not unique. As can be seen from Figure 3, two pairs of distances, i.e. the $F_e..F_e$ and O..O distances in the equatorial plane and the $F_a..F_e$ and $F_a..O$ distances between axial and equatorial substituents can be interchanged. The former interchange leads to an F_e-Os-F_e angle smaller than or nearly equal to the O=Os=O angle and the latter interchange to F_e-Os-F_a angles smaller or larger than the $O=Os-F_a$ angles. The equatorial $F_e-Os=O$ angles are nearly unaffected by thes interchanges. While all four possible assignments for the 2.56-Å peak components fit the experimental radial distribution curve and the molecular intensities nearly equally well, only one assignment is in accord with our theoretical calculations (see below) and general VSEPR arguments.[39] On the basis of these, the osmium–oxygen bonding domains are more repulsive than the osmium–fluorine domains and, therefore, the O–Os–O bond angle must be larger than the equatorial F–Os–F angle, and the axial fluorine atoms must be bent away from the oxygen ligands. Using this constraint for the bond angles and the resulting assignments for the individual components of the 2.56-Å peak of the radial distribution curve, the diffraction data were refined for both, model I and model II, and resulted in a slightly lower (by 8%) *R*-factor for model II (see Table I). Since the vibrational amplitude for the short nonbonded distances causes high correlations in the least-squares analysis, this amplitude was not refined. When five geometric parameters [r(Os–O), $r(Os-F)_{mean}$, ∠OOsO, $\angle F_eOsF_e$, $\angle F_eOsF_a$] and three vibrational amplitudes were refined simultaneously, only one correlation coefficient had a value larger than |0.5|: $F_eOsF_e/OOsF_a = -0.79$. Of the two structural models for OsO_2F_4, model II (Figure 4) is preferred since it results in the lowest *R*-factor and because theoretical calculations of the type used in our study are known to reproduce differences between bond lengths of similar types, such as $Os-F_e$ and $Os-F_a$, very well.

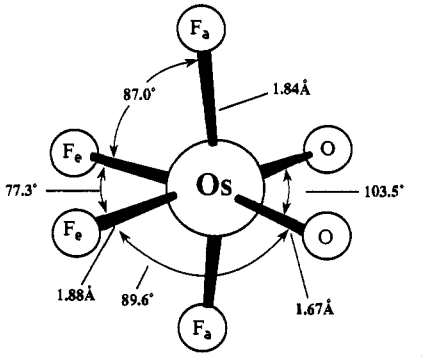

Figure 4. Molecular structure of gaseous *cis*-OsO_2F_4 from combined electron diffraction and computational data.

A comparison of the structure of *cis*-OsO_2F_4 with those of OsO_4,[40] $OsOF_4$,[41] and OsF_6[42] shows the following trends:

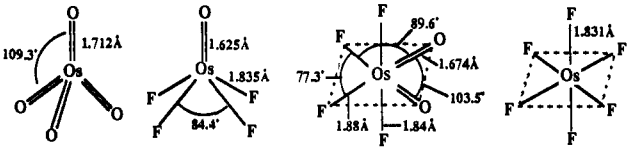

The Os–O bond length increases with an increasing number of oxygen ligands; i.e., oxygen releases electron density to the high oxidation state osmium central atom. This allows the transfer of more negative charge to the remaining ligands, thereby increasing the polarities and lengths of these bonds. The Os–F bond length also increases with increasing oxygen substitution; i.e., it increases from 1.835(7) Å in $OsOF_4$ to an average of 1.863(3) Å in *cis*-OsO_2F_4. Obviously, secondary effects, such as the formal oxidation state of the central atom and its coordination number, will also contribute to the bonding but cannot be analyzed at the present time in the absence of more precise data and further examples.

(38) Haase, J. *Z. Naturforsch., A* **1970**, *25*, 936. The problems of possibly inadequate scattering amplitudes or phases for atoms of high atomic number and the importance of multiple scattering have recently been studied extensively for the tantalum compound $(CH_3)_3TaF_2$, which also contains a sixth row element (Elbel, S.; Oberhammer, H. To be published). It was found that these possible inadequacies in scattering theory have a negligible effect on geometric parameters and lead to small changes in vibrational amplitudes only.

(39) (a) Gillespie, R. J. *Molecular Geometry*; Van Nostrand Reinhold: London, 1972. (b) Gillespie, R. J.; Hargittai, I. *The VSEPR Model of Molecular Geometry*; Allyn and Bacon: Boston, 1991.

(40) Seip, H. M.; Stolevik, R. *Acta Chem. Scand.* **1966**, *20*, 385.

(41) Alekseichuk, I. S.; Ugarov, V. V.; Rambidi, N. G.; Legasov, V. A.; Sokolov, V. B. *Proc. Acad. Sci. USSR (Engl. Transl.)* **1981**, *257*, 99.

(42) Weinstock, B.; Claassen, H. H.; Malm, J. G. *J. Chem. Phys.* **1960**, *32*, 181. Claassen, H. H.; Goodman, G. L.; Kimura, M.; Schomaker, V.; Smith, D. W. *J. Chem. Phys.* **1968**, *48*, 4001.

Table II. Vibrational Spectral Data for *cis*-OsO_2F_4

assgnts and approx mode descriptions in point group C_{2v}			obsd[a] freq, cm^{-1} (rel int)		calcd freq, cm^{-1} (IR int)	
			IR (25 °C)	R (−150 °C)	NLDFT/BP[b]	LDFT[c]
A_1 (IR, R)	ν_1	ν_{sym} OsO_2	940 s	943 (100)	947 (78)	918 (79)
	ν_2	sym comb of sym ax and sym equat OsF_2 stretch		673 (59)	648 (47)	663 (50)
	ν_3	antisym comb of sym ax and sym equat OsF_2 stretch	590 vs	580 (17)	578 (24)	595 (33)
	ν_4	δ_{sciss} OsO_2		402 (38)	376 (1.3)	374 (5.4)
	ν_5	sym comb of ax and equat OsF_2 scissor		350 (31)	321 (6.0)	325 (13)
	ν_6	antisym comb of ax and equat OsF_2 scissor		217 (1)	212 (1.5)	212 (2.2)
A_2 (-, R)	ν_7	OsO_2 torsion		314 (1)	321 (3.9)	322 (14)
	ν_8	OsF_{2e} torsion		95 sh	100 (0)	95 (7.7)
B_1 (IR, R)	ν_9	ν_{as} OsF_{2a}	680 vs	680 sh	676 (198)	690 (203)
	ν_{10}	δ_{rock} OsF_{2a}		323 (1)	325 (7.8)	326 (11)
	ν_{11}	δ_{rock} OsF_{2e}		266 (2)	269 (38)	268 (35)
B_2 (IR, R)	ν_{12}	ν_{as} OsO_2	930 s	933 (31)	950 (111)	929 (110)
	ν_{13}	ν_{as} OsF_{2e}	570 vs	572 (14)	553 (43)	576 (26)
	ν_{14}	sym comb of $OOsF_e$ sciss and OsF_{2a} sciss		344 (31)	311 (20)	317 (25)
	ν_{15}	antisym comb of $OOsF_e$ sciss and OsF_{2a} sciss		168 (3)	181 (0.4)	176 (0.5)

[a] In addition to the bands listed, the following very weak Raman bands were observed: 246 (1) = (168 + 79), 190 (O+), 175 sh, 79 (1) = lattice vibration. [b] Unscaled frequencies. [c] The stretching frequencies were scaled by an empirical factor of 0.9424 to maximize their agreement with the observed ones.

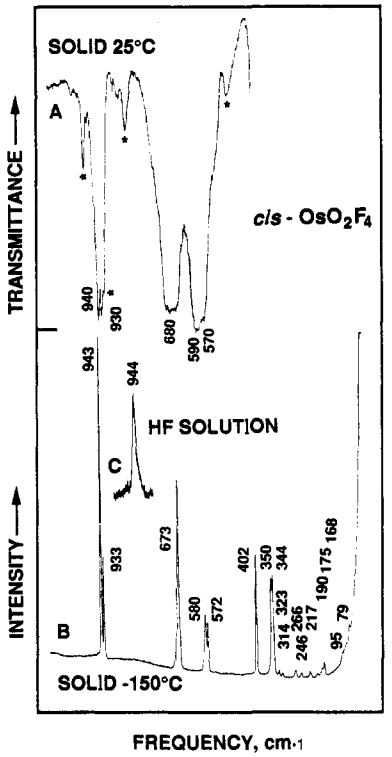

Figure 5. Infrared (A) and Raman (B and C) spectra of *cis*-OsO_2F_4 in the solid state (A and B) and HF solution (C). The bands marked by an asterisk are due to decomposition products.

Vibrational Spectra. The infrared and Raman spectra of solid OsO_2F_4 and the Raman spectrum of its HF solution are shown in Figure 5. The observed frequencies, together with their assignments in point-group C_{2v}, are listed in Table II. The assignments were made by comparison with the calculated frequencies and intensities (see Table II and below) and are unambiguous for the seven fundamental vibrations with the highest frequencies, i.e., for the bands above 400 cm^{-1}. In the 300–350-cm^{-1} region, four Raman bands were observed at 350, 344, 323, and 314 cm^{-1}, which must be assigned to $\nu_5(A_1)$, $\nu_7(A_2)$, $\nu_{10}(B_1)$, and $\nu_{14}(B_2)$. Of these, $\nu_5(A_1)$ and $\nu_{14}(B_2)$ involve very similar type of motions and, by comparison with the related SF_4 [43] and PF_4^- [44] species, should be of much higher Raman intensities than the OsO_2 rocking and the OsO_2 torsion motions. Therefore, $\nu_5(A_1)$ and $\nu_{14}(B_2)$ were assigned to the Raman bands at 344 and 350 cm^{-1}, respectively, and $\nu_7(A_2)$ and $\nu_{10}(B_1)$ to 314 and 323 cm^{-1}, respectively. In the 200–270-cm^{-1} region, three bands were observed at 217, 246, and 266 cm^{-1}, two of which should belong to the OsF_{2eq} rocking mode, $\nu_{11}(B_1)$, and the antisymmetric combination of axial and equatorial OsF_2 scissoring, $\nu_6(A_1)$. Since the 246-cm^{-1} band has the lowest Raman intensity and can be assigned to a combination band, i.e., 168 + 79 = 247 cm^{-1}, the 266-cm^{-1} Raman band was assigned to $\nu_{11}(B_1)$ and the 217-cm^{-1} one to $\nu_6(A_1)$. The remaining yet unassigned modes, $\nu_{15}(B_2)$ and $\nu_8(A_2)$, have calculated frequency values of about 176 and 95 cm^{-1}, respectively, and consequently are assigned to the Raman bands observed at 168 and 95 cm^{-1}, respectively, leaving only two very weak Raman features at 190 (0+) and 175 (sh) cm^{-1} and a probable lattice vibration at 79 cm^{-1} unassigned. Although the assignments below the 344-cm^{-1} Raman line are somewhat

Table III. Calculated Structure and Vibrational Frequencies for OsO_4

Bond Distances (Å)			
	LDFT	NLDFT/BP	expt
r(Os–O)	1.730	1.739	1.71

Vibrational Frequencies (cm^{-1}) and IR Intensities (km/mol)			
sym	expt	LDFT	NLDFT/BP
A_1	965	1000 (0)	953 (0)
E	333	292 (0)	323 (0)
F_2	960	1027 (359)	980 (329)
	329	300 (16)	339 (10)

Table IV. Geometry Parameters[a] for OsO_2F_4

	C_{2v} (*cis*) (see Figure 4)		C_{2v} (*trans*) (see Figure 6)		
	LDFT	NLDFT/BP	LDFT	NLDFT/BP	expt
r(Os–O)	1.724	1.735	1.734	1.741	1.674(4)
r(Os–F)	1.881 a	1.902 a	1.882 e2	1.900	1.843(3) a
r(Os–F)	1.921 e	1.944 e	1.927 el	1.965	1.883(3) e
∠O–Os–O	102.6	102.1	137.2	136.9	103.5(25)
∠O–Os–F	89.4 e	89.4 e	106.9 e2	106.9	89.6(16) e
∠O–Os–F	94.1 a	93.8 a	81.0 el	80.9	92.4(17) a
∠F–Os–F	169.0 a,a	167.7 a,a	129.7 el,el	129.2	172.0(35) a,a
∠F–Os–F	78.6 e,e	79.1 e,e	75.2 e2,e2	75.5	77.3(26) e,e
∠F–Os–F	85.0 a,e	85.3 a,e	77.5 el,e2	77.6	87.0(15) a,e

[a] Bond distances in Å. Bond angles in deg.

(43) Christe, K. O.; Willner, H.; Sawodny, W. *Spectrochim. Acta, Part A* **1979**, *35A*, 1347 and references cited therein.

(44) Christe, K. O.; Dixon, D. A.; Mercier, H. P.; Sanders, J. C. P.; Schrobilgen, G. J.; Wilson, W. W. Submitted for publication in *J. Am. Chem. Soc.*

Table V. Vibrational Frequencies (cm^{-1}) and IR Intensities (km/mol) for C_{2v} *trans*-OsO_2F_4

sym	LDFT	NLDFT/BP	sym	LDFT	NLDFT/BP
A_1	955 (18)	925 (30)	B_1	968 (132)	950 (97)
	726 (82)	672 (87)		345 (4.9)	336 (2.8)
	589 (18)	527 (20)		256 (3.3)	255 (2.5)
	403 (7.0)	385 (2.5)	B_2	706 (159)	638 (142)
	333 (12)	321 (15)		594 (5.6)	537 (5.2)
	122 (0.4)	117 (0.8)		304 (14)	299 (15)
A_2	419 (0.2)	407 (0)		241 (21)	230 (20)
	96 (3.8)	89 (0)			

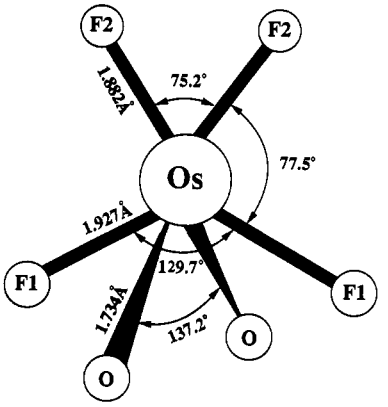

Figure 6. Minimum energy C_{2v} structure of OsO_2F_4 obtained from the *trans*-D_{4h} structure as a starting point in the LDFT calculation. The Os, F1, and F2 atoms are all in one plane.

tentative, the agreement with the calculated frequencies and anticipated intensities is quite good (see Table II). Hence, the observed vibrational spectra strongly support the pseudooctahedral *cis*-structure established by both the electron diffraction and the NMR studies.

Computational Results. The geometries and vibrational spectra of *cis*- and *trans*-OsO_2F_4 were calculated using density functional theory at the local density functional (LDFT) level with the local potential of Vosko et al.[22] and also at the nonlocal level with the exchange potential of Becke[23] together with the nonlocal correlation functional of Perdew[24] (NLDFT/BP). To test the accuracy of these methods, the well-known OsO_4 molecule[40] was first calculated. The results are summarized in Table III. As can be seen, the calculated bond lengths are slightly longer than the observed one, but the calculated frequencies and, in particular those at the NLDFT/BP level, are quite close to the experimental ones even without scaling.

The calculations for *cis*- and *trans*-OsO_2F_4 (see Tables II, IV, and V) show that the *cis*-structure for OsO_2F_4 is a true minimum. The D_{4h} *trans*-structure is not a minimum energy structure and distorts to a C_{2v} structure as shown in the Figure 6. The minimum-energy structure is 17.7 kcal/mol lower in energy as compared to the minimum-energy C_{2v} *trans*-structure at the local DFT level and is 15.5 kcal/mol lower in energy than the *trans*-structure if nonlocal correlations are included. The fact that contrary to $IO_2F_4^-$, which exists as both a *cis*- and *trans*-isomer,[45] OsO_2F_4 forms only a stable *cis*-isomer is in accord with previous conclusions[46-48] that in octahedral dioxo complexes, MO_2X_4, metals with a d^0 configuration prefer a *cis*-structure.

Acknowledgment. The work at Rocketdyne was financially supported by the U.S. Air Force Phillips Laboratory and the U.S. Army Research Office, while that at McMaster University was supported by the U.S. Air Force Phillips Laboratory and the Natural Sciences and Engineering Research Council of Canada. The authors thank Drs. W. W. Wilson, C. J. Schack, and R. D. Wilson of Rocketdyne for helpful support.

Note Added in Proof. After completion of this work, two publications dealing with OsO_2F_4 appeared. In the first one (*Chem. Ber.* **1993**, *126*, 1331) Bougon, Buu, and Seppelt report a crystal structure. Their results were severely hampered by absorption and disorder problems and, therefore, did not yield a reliable geometry for OsO_2F_4. In the second paper (*Chem. Ber.* **1993**, *126*, 1325) Veldkamp and Frenking report the results from ab initio calculations at the HF and MP2 levels of theory. A comparison of their results with ours shows that our density functional theory calculations reproduce the experimental values much better and, therefore, should be preferred.

(45) Christe, K. O.; Wilson, R. D.; Schack, C. J. *Inorg. Chem.* **1981**, *20*, 2104.
(46) Griffith, W. P.; Wickins, T. D. *J. Chem. Soc. A* **1968**, 400.
(47) Griffith, W. P. *J. Chem. Soc. A* **1969**, 211.
(48) Hope, E. G.; Levason, W.; Ogden, J. S. *J. Chem. Soc., Dalton Trans.* **1988**, 997.